Simple Raman Spectroscopic System Coupled with Ag Nanostar Colloid as SERS Substrate for Detection of Low Concentrations of Water Pollutants

Zinah S. Shakir [1,2]
Ayad A. Dhaigham [3]
Sameer K. Yaseen [4]

[1] *Institute of Laser for Postgraduate Studies, University of Baghdad, Baghdad, IRAQ*
[2] *Department of Applied Sciences, University of Technology, Baghdad, IRAQ*
[3] *Directorate of Materials Research, Ministry of Science and Technology, Baghdad, IRAQ*
[4] *Department of Physics, College of Science for Women, University of Baghdad, Baghdad, IRAQ*

Raman spectroscopy is considered an effective characterization tool for the quantitative detection of pollutants in water, especially when coupled with surface enhanced Raman scattering (SERS) technique. SERS is a highly sensitive and selective approach; it improves Raman signals by using nano-materials as substrates. In this study, a low-cost Raman detection system was designed, manufactured, and integrated with SERS technique using a star-shaped nanosilver (AgNS) colloidal solution as a liquid substrate to enhance Raman detection at low concentrations of pollutants. The AgNS colloid was synthesized from silver ions using a chemical reduction method. Sodium nitrate solutions with various concentrations were used as water pollutants. Using SERS technique, the results showed a noticeable improvement in the Raman signal of the sodium nitrates' spectra samples. The highest analytical enhancement factor for SERS was 7.48 for the sample of the lowest concentration (0.05M) of sodium nitrates.

Keywords: Localized surface plasmon; Raman spectroscopy; Raman scattering; Silver nanostars
Received: 14 September 2023; **Revised:** 21 November 2023; **Accepted:** 28 November 2023

1. Introduction

Raman spectroscopy is a widely used technique to identify the physicochemical properties of materials in their solid, liquid, and gaseous states by analyzing the vibrational properties of molecules or ions [1]. The Raman phenomenon was first discovered by the Indian physicist Raman in 1928. It defines the inelastic scattering of the photons that irradiate materials as Raman scattering is generated when electrons of a material interact with the electromagnetic radiation in a unique way resulting in a nuclei movement. It involves a virtual state, where a photon and a molecule co-exist for an incredibly short amount of time. This energy state is considered a collective state of both photons and molecules. The Raman scattering process can be categorized into three types: Rayleigh, Stokes, and anti-Stokes, as illustrated in Fig. (1).

Raman scattering is a two-photon process that involves a virtual state [2,3]. As illustrated in Fig. (1a), Rayleigh scattering is an elastic scattering, a process in which the energy of the initial and the final states are equal. In contrast, Stokes and anti-Stokes scattering are inelastic scatterings, (see Stokes scattering process depicted in Fig. 1b), which occurs when energy transfer from the photon to the molecule exists in the ground state, leading to an excited quantum state. Anti-Stokes scattering occurs when energy transfers from the photon to the molecule are initially in an excited quantum state, resulting in the scattering process ending in the ground state; see Fig. (1c). This transfer of energy from the molecular quantum system to the photon is the hallmark of this process. In vibrational Raman spectroscopy, the quantum states depicted in Fig. (1) refer to the vibrational levels. According to the Boltzmann distribution, the vibrational ground state is more heavily populated than the energetically excited vibrational states at room temperature. Therefore, the intensity of the Stokes Raman scattering typically exceeds that of the anti-Stokes Raman scattering [2,4,5]. Since the molecules of each substance have a specific vibrational spectrum, it is possible to measure the concentration of multiple substances with a single measurement and provide chemical information about all the substances present in the sample at once and in a short time. Thus, anions-containing compounds like NO_2, NO_3, PO_4, SO_4, and HPO_4 may be recognized using Raman spectroscopy [6]. By calibrating the Raman scattering intensity for known amounts of Reference materials, quantitative measurements of ion concentrations in water can be achieved [7]. However, applying this approach as a quantitative probe of materials is not straightforward and requires several careful steps, including appropriate calibration process and spectrum normalization [8].

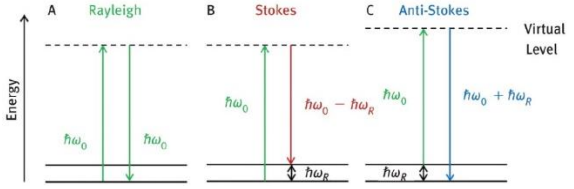

Fig. (1) Schematic energy diagrams of Rayleigh, Stokes, and anti-Stokes Raman scattering

Raman spectroscopy offers many benefits; it is versatile and can analyze a wide range of materials, including solids, liquids, polymers, and vapors, without the need for sample preparation. Furthermore, it is not affected by water, making it an ideal choice for many applications. It is also non-destructive, highly specific, and can provide a unique "fingerprint" of each material. Spectra can be obtained quickly, often in just a few seconds, and can even be acquired through glass or polymer packaging. Optical fibers can be used to transmit scattered Raman light over long distances for remote analysis. With Raman spectroscopy, a wide range of frequencies can be covered by a single recording. In addition, Raman spectra can be obtained from very small amounts of materials, making them particularly useful for analyzing inorganic materials [9,10].

Although Raman spectroscopy has a very high molecular selectivity, the weak spontaneous Raman scattering effect is a significant limitation of Raman spectroscopy, i.e., its sensitivity is very low since only one photon out of 10^8 incident photons is typically scattered inelastically, producing Raman signal [2]. However, the weak cross-section of Raman scattering can be enhanced by some orders of magnitude utilizing several techniques such as surface enhanced Raman scattering (SERS) [7]. SERS is a technique that enhances the typically weak Raman signals by adsorbing molecules to be detected on a roughened surface of metal or metal nanoparticles [11]. It is a highly sensitive technique that is capable of detecting a single molecule and achieving very large enhancement factors with appropriate metal nanostructures, particularly free-electron metals like gold, silver, and copper [12,13]. SERS substrates can either be colloidal nanoparticles in solution or nanostructures that have been placed on a surface [3]. These metal nanostructures increase the Raman spectral signature of molecules deposited on them by electromagnetic motivation in regions that are often nanogaps between adjacent metal nanostructures or narrow areas surrounding the tips of metal nanostructure on the SERS substrate. These regions are called 'hot spots' [14,15]. It has been found through previous research that hot spot amplification increases to the greatest extent when the size of nanoparticles decreases, the distance between them shortens, and the surface curvature increases [16], see Fig. (2).

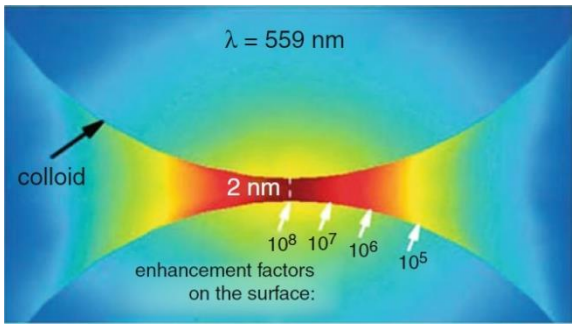

Fig. (2) The various hotspot amplifications that formed between two closely placed nanoparticles resulting from a coupled Plasmon resonance [19]

In the field of Raman spectrometry, the excitation source plays a crucial role in delivering a powerful and highly monochromatic light. The bandwidth and the power of the excitation source are the most important considerations for achieving optimal Raman spectroscopy results. As such, a narrow bandwidth or a highly monochromatic beam with high power is preferred for achieving optimal stability and intensity of the Raman spectrum. Lasers are the most commonly used excitation sources due to their ability to deliver a highly-monochromatic beam with sufficient power density. It is worth noting that the frequency shift between the excitation signal and the induced Raman signal is directly influenced by the fundamental vibrational frequency of the molecule [17].

The range of available wavelengths spans from ultraviolet (UV) to near-infrared (NIR). When performing Raman spectroscopy on a particular sample, it is necessary to carefully consider the wavelength of light utilized in the excitation process. The selection of an appropriate laser wavelength should be based on the likelihood of sample fluorescence or degradation, as the laser wavelength should not be within the absorption spectrum of the sample. Longer wavelength excitation lasers provide less energy to the sample, resulting in a lower Raman virtual state, which is less likely to interfere with the higher electronic state and is consequently, less likely to cause fluorescence [18]. However, employing a longer wavelength excitation laser can also lead to a reduction in the efficiency of Raman scattering, which is defined by Eq. (1) where λ represents the excitation wavelength [19].

$$\text{Raman efficiency} = \frac{1}{\lambda^4} \quad (1)$$

It is worth noting that according to the efficacy equation, using UV Raman region with wavelengths below 400 nm can generate up to 100 times stronger Raman scattering signals than that when using visible light. UV Raman can also eliminate background fluorescence. However, UV Raman is a complicated and expensive technique, potentially degrading the sample. Hence, 532 nm and 780 nm lasers are most commonly used to analyze carbon-based materials, as

they produce efficient Raman scatters and are less prone to fluorescence [20].

In this work, we aim to design and manufacture a simple Raman spectroscopy device coupled with SERS technique by the use of star-like silver nanostructure as a liquid SERS substrate to enhance a Raman signal that can effectively detect low concentrations of sodium nitrate as a pollutant in water.

2. Experimental Part

Silver nitrate ($AgNO_3$), hydroxylamine (HA) solution (50 w/w in water), tri-sodium citrate (TSC), and sodium hydroxide (NaOH) solutions were prepared in double-ionized water. The first step to prepare the silver nanostar colloid was mixing 1mL of HA 6×10^{-2} M with 1mL of NaOH 0.05 M. Then, 20 mL of $AgNO_3$ 10^{-3} M was added dropwise to the solution under agitation. After 5 minutes, 200 µL of TSC 4×10^{-2} M (1%, w/v) was added to the mixture, and the final suspension was stirring for 15 min with a magnetic stirrer before measuring a pH of 5.5 [21]. To examine the Ag nanostar colloid, an FEI Inspect f50 field-emission scanning electron microscopy (FE-SEM) and x-ray diffractometer (XRD) were employed.

The samples were prepared by dissolving ($NaNO_3$, 99%, supplied by Sabik, KSA), in distilled water at concentrations of 0.1, 0.4, 0.7, and 1 M at room temperature and atmospheric pressure.

Four samples of sodium nitrate were prepared in the colloidal AgNS instead of distilled water at concentrations of 0.05, 0.1, 0.5, and 1 M at room temperature and atmospheric pressure.

The probe optics configuration used in this experiment was backscattering, as it is the easiest to set up and only requires a few components and alignment.

A MGL-111-532-100mW CW diode-pumped solid-state laser (DPSS) providing monochromatic light at 532 nm, and output power range of 0-100 mW was utilized as the excitation source. An Ocean Optics HR2000 high-resolution spectrometer with a spectral resolution of 2 cm^{-1}, was employed as the detector (see Fig. 3b).

The necessary backscattering configuration was obtained by using various optical elements, including a band-pass filter (BP) to transmit only a certain wavelength region of the electromagnetic wave of the excitation source (532 nm), a dichroic beam splitter (DBS) positioned at 45° to the laser light path to direct the path of the excitation beam toward the sample, and then pass the backscattered Raman radiation from the sample toward the detector, a notch filter (NF) for blocking out intense Rayleigh scattered radiation that could otherwise interfere with the detector's readings, and a collimating lens with a focal length of 5cm to collect and focus the beam inside the sample, along with three concave mirrors to collect dispersed rays. Additionally, an optical microscope was employed to focus the passing rays to the detector, and a fiber optic cable was used to transmit the obtained signal to the detector (see Fig. 3a).

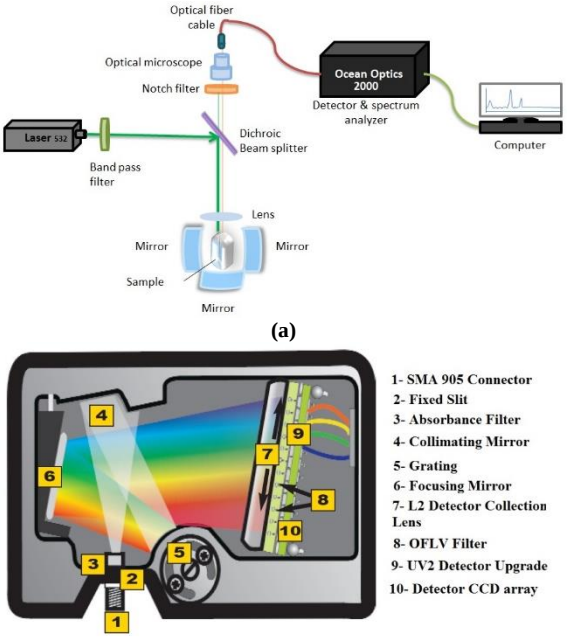

Fig. (3) Raman spectroscopic system (a) Schematic overview of Raman spectroscopy, (b) Definition of Ocean 2000 spectrometer

To ensure accurate results, it is important to ensure that the material to be examined has an absorption spectrum that is far from the emission spectrum of the excitation source, as this prevents the occurrence of fluorescence that can obscure the Raman signal during the test. First, we checked the absorbance of the analyte using an UV-visible spectrophotometer. Then, the samples were subjected to Raman test. All of the measurements were done at room temperature.

Aqueous solutions of $NaNO_3$ samples at concentrations of 0.1, 0.4, 0.7, and 1 M for regular Raman examination at concentrations of 0.05, 0.1, 0.5, and 1 M for SERS examination were added separately into glass cuvettes with a volume of 3 mL, and dimensions of 10x10x45mm. They were then individually irradiated with a laser power of 70 mW for 10 s per sample. In all cases, the integration time was adjusted to 9 ms. Results were compared with the typical spectrum of the substance.

3. Results and Discussion

Based on the data presented in Fig. (4), it appears that the absorption spectrum of $NaNO_3$ is distributed over a range of approximately 270-350nm. This suggests that the laser used in the excitation process is well-suited for the test, as it operates at a wavelength that is not in close proximity to the absorbance area that produces fluorescence. In the fluorescence process, the energy of the source must

exactly match the energy difference between the ground and first excited electronic states for absorption to take place, so the ground and first excited electronic states are called quantized. Disparity in energy between the two electronic states also controls the energy of a photon that is released. While in the Raman scattering process, the transmission happens in a virtual electronic state which is not quantized and is determined by the energy of the radiation source [22]. Therefore, the radiation source doesn't need to coincide with a specific change in energy. Without changing its vibrational energy state, the analyte transitions from its ground electronic state to a virtual electronic state upon absorbing a photon of source radiation.

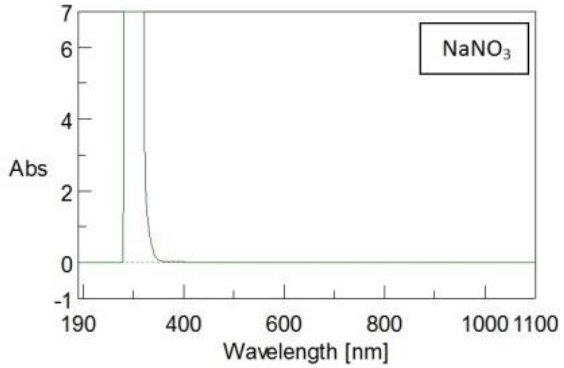

Fig. (4) Absorption spectrum of $NaNO_3$

The careful preparation and testing process ensured that the data was reliable and accurate. When quantifying the intensity of a vibrational mode in Raman spectroscopy, it is important to first extract the true signal and subtract the background. Normalizing the intensity of the peak is also necessary, but can be tricky due to fluctuations in the laser source power or detector. To avoid systematic errors in concentration determination, a peak sensitive to these variations and independent of the substance under study should be used as a reference in the spectrum.

Normal Raman spectrum of sodium nitrate solution at concentration 1M is shown in Fig. (5). A very intense and broad line in the range 3000-3800 cm^{-1} representing the OH stretching bond, also a small peak at 1632 cm^{-1} due to the H-OH bending bond were detected. There is a sharp and intense peak at 1051 cm^{-1} due to the symmetric stretching (ν_1) mode of the nitrate ion. Moreover, two weak peaks were detected at 1379 and at 723 cm^{-1} corresponding to asymmetric stretching (ν_3) and in-plane bending (ν_4) modes of nitrate ion respectively [23]. The obtained spectra are very close to the typical ones.

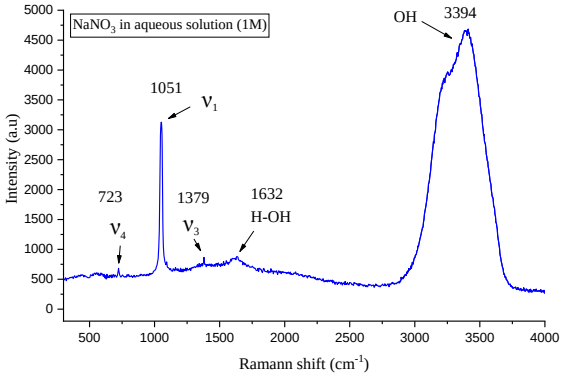

Fig. (5) Raman shift of the aqueous solutions of $NaNO_3$ at concentration 1M

We can see from the results that the sharp intense peak of ν_1 mode becomes weaker as the concentration of nitrate decreases in the aqueous solution. Also with decreasing the concentration, modes ν_3 and ν_4 disappeared, as shown in Fig. (6a,b). The intensity of the symmetric stretching ν_1 mode of NO_3 molecule in sodium nitrate solution is considered to be the specific and relevant signature of nitrate ion and can be studied as a function of concentration of analyte; see Fig. (7). A Raman sensor can also be used to determine the content of different species in a mixture based on the fact that the Raman intensity is directly proportional to the number of active molecules in the scattered cross section [24].

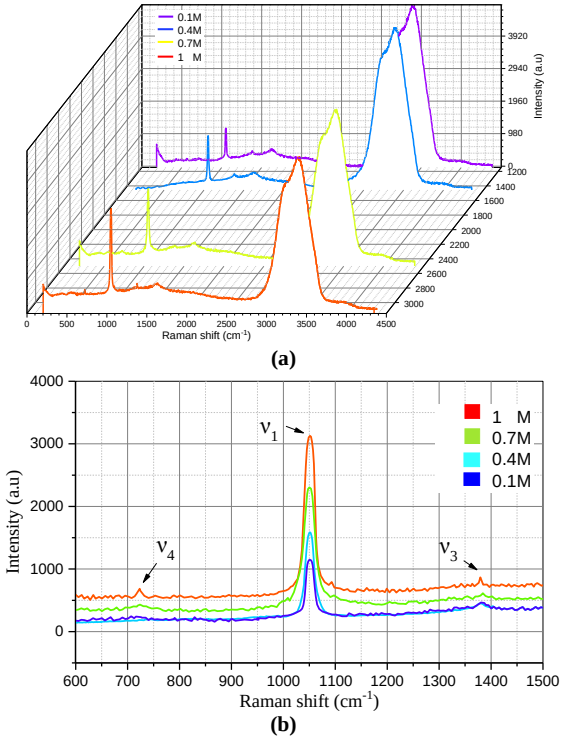

Fig. (6) Normal Raman spectra of $NaNO_3$ in aqueous solutions with variable concentrations, (a) The whole spectra range of the aqueous solutions (b) Raman shift of the NO_3 vibration modes only

According to the FE-SEM image, the approximate size of the nanostars was 60 nm. The nanostars seem

to be agglomerated and clustered on top of each other forming hotspots as shown in Fig. (8).

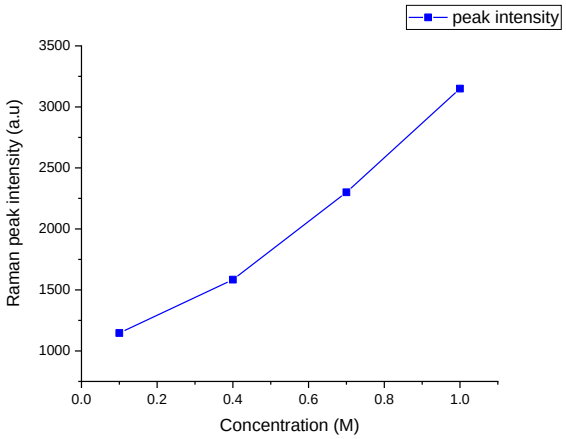

Fig. (7) Concentrations of $NaNO_3$ in aqueous solution versus the normal Raman peak intensity of the symmetric stretching ν_1 mode of NO_3 molecule in sodium nitrate solutions

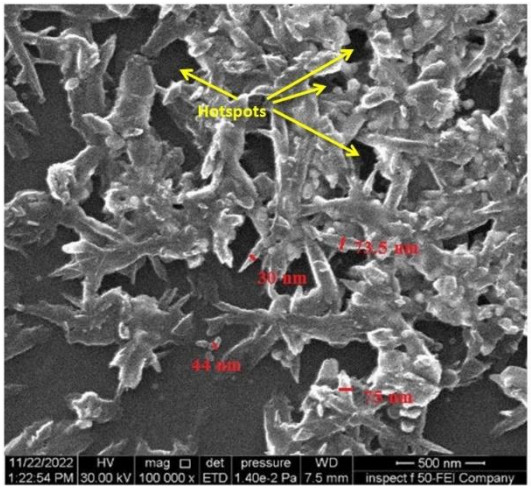

Fig. (8). FE-SEM image of silver nanostars showing hotspots between nanostructures and the average size of the nanostars

The X-ray diffraction pattern of the AgNS structure showed some interesting diffraction peaks at 38°, 64.4°, and 77.5°, which are very similar to pure silver crystal planes (111), (220), and (331). As depicted in Fig. (9), these strong peaks in the planes suggest that the AgNSs are highly crystalline. It is worth mentioning that there were no additional impurity peaks found, indicating that the samples were very pure.

From the results of SERS samples as shown in Fig. (10a,b), we can see a significant enhancement in the main peak of nitrate (ν_1). In analyzing the SERS $NaNO_3$ samples, it was found that their Raman intensities were greater at all Raman peaks than the normal ones.

The Raman signal is simultaneously amplified through both the electromagnetic mechanism (EM) and chemical mechanism (CM), which are the components of the SERS effect. The EM enhancement is influenced by the local increase in the electric field adjacent to the nanoparticles caused by the localized surface plasmon resonances (LSPR) [11]. As for the CM mechanism, the charge-transfer interactions between the nanoparticle surfaces and the electronic states of the molecules give rise to the CM, which will also lead to a rise in Raman signals. As a result, the EM depends on LSPR, whereas the CM is determined by the Raman-active molecule and its interactions with the surface of the nanoparticle [25].

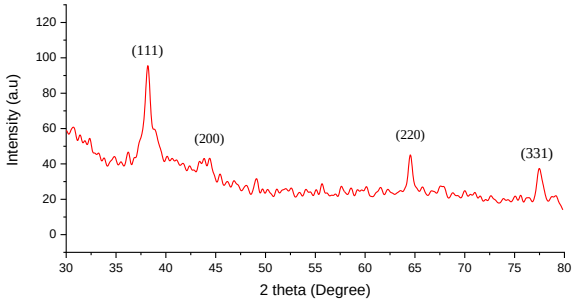

Fig. (9) The XRD pattern of AgNSs synthesized in this work

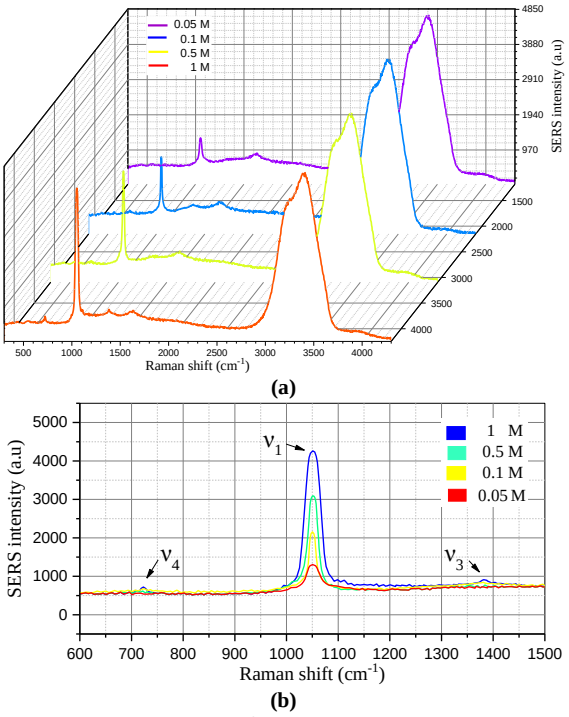

Fig. (10) SERS spectra of $NaNO_3$ diluted in Ag nanostar colloids with various concentrations, (a) The whole SERS spectra range of the aqueous solutions (b) SERS spectra of the NO_3 vibration modes only

It appears that when the nitrate molecules, embedded in the hotspots generated by the aggregation of Ag nanostructures and the sharp edges of the nanostars, are exposed to laser light, a localized surface plasmon (LSP), linked to collective oscillations of the electron cloud within nanostructures excites the local electromagnetic field which is created around the hotspots [13, 26-28]. This excited local electromagnetic field, which is up to 100 times stronger than the incident one, results in a significant amplification of the Raman signal, and

due to the adjacency effect, the enhancement is stronger when the nanoparticles are aggregated rather than individual [3].

The correlation between the $NaNO_3$ concentrations in the silver nanocolloidal and the SERS intensity was depicted in Fig. (11). It is evident that as the nitrate concentration rises, so does the SERS intensity. This is because there are more nitrate molecules coupled to AgNSs, which strengthens the Raman signal and improves Raman scattering [11,25].

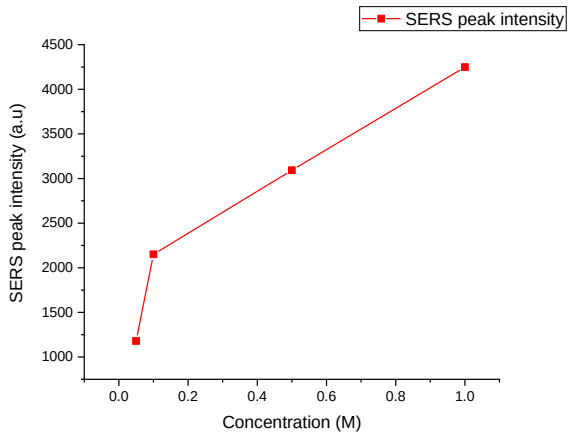

Fig. (11) SERS peak intensities of the symmetric stretching ν_1 mode of NO_3 molecules in sodium nitrate diluted in Ag nanostar colloid versus the nitrate concentrations

One of the most crucial parameters used to assess a substrate's ability to boost the Raman signal for SERS applications is the determination of the SERS analytical enhancement factor (AEF) [29]. It is an analytical approach of signal enhancement, combines signal intensity with the concentration of analyte. This measurement is helpful when it's difficult to estimate the number of analyte molecules present, particularly for analytes that don't have a strong affinity for the plasmonic surfaces. In the SERS approach, AEF is proportional to the intensity of the "hot spot" [11,29]. The analytical enhancement factor of an analyte is:

$$AEF = \frac{I_{SERS} \times C_{NRS}}{C_{SERS} \times I_{NRS}} \quad (2)$$

where I_{NRS} is the normal Raman intensity, I_{SERS} is the SERS intensity, C_{NRS} is the analyte concentration in the normal Raman, and C_{SERS} is the concentration of the analyte in the SERS liquid substrates.

The AEF against various sodium nitrate solution concentrations was plotted in Fig. (12), where it shows a non-linear rise in AEF as the nitrate content decreases. The maximum nitrate AEF was 7.48 at the lowest concentration (0.05M), which means that SERS has higher efficiency with lower concentrations. When molecules are present in trace amounts, the electric field of the target molecule located in the hot spot will rise locally, enhancing the SERS signal and thus raising the AEF. The aggregation of the silver nanoparticles plays a main role in the enhancement factor value, where the AEF is proportional to the local electromagnetic field's strength (a hotspot). The properties of metal nanoparticle colloids depend on how the metal and molecules interact with each other. This interaction affects the overlap between the laser source and SPR bands, which can vary based on the size and edges of the nanoparticles. This difference is primarily responsible for differences in AEF.

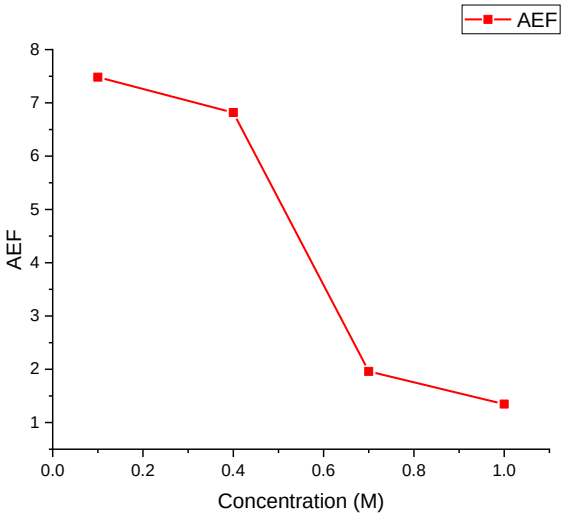

Fig. (12) The dependence of SERS analytical enhancement factor on the concentration of $NaNO_3$ in AgNS at the symmetric stretching ν_1 mode of NO_3 molecules in sodium nitrate diluted in Ag NS colloid

4. Conclusion

A compact spectrophotometer system, coupled with colloidal AgNS as liquid SERS substrate has been designed and constructed for detecting low concentrations of pollutants in water. Sodium nitrate solutions with various low concentrations were detected as a pollutant. There is an increase in Raman shift peaks' intensities of the nitrate spectrum with the increase of the nitrate content of the sample. Hotspots, which originated due to the accumulation of AgNSs in the sample solution, have the effect of intensifying the electromagnetic fields around them. The analytical enhancement factor is proportional to the magnitude of the local electromagnetic field at the nitrate molecule. Finally, it was found that the SERS technique is more effective at lower concentrations of the detected material, where the highest enhancement factor value observed when detecting $NaNO_3$ samples was 7.48 at the lowest concentration of nitrate (0.05M).

References

[1] M.Q. and T.A.A. Hassan, “Magnéli Phase Titanium Sub-Oxide Production using a Hydrothermal Process”, *Karbala Int. J. Mod. Sci.*, 8(4) (2022) 651-656.

[2] D. Cialla-May, M. Schmitt and J. Popp, "Theoretical principles of Raman spectroscopy", *Phys. Sci. Rev.*, 4(6) (2019).

[3] R. Gillibert et al., "Explosive detection by Surface Enhanced Raman Scattering", *TrAC Trends in Anal. Chem.*, 105 (2018) 166-172.
[4] C.L. Sanford, B.A. Mantooth and B.T. Jones, "Determination of Ethanol in Alcohol Samples Using a Modular Raman Spectrometer", *J. Chem. Edu.*, 78(9) (2001) 1221-1225.
[5] O.A. Hamadi "Instrumentation of absorption spectrum of an NH_3-filled cell to IR laser pulses using cavity-ring down technique", *Proc. SPIE*, 5776 (2005) 479-484.
[6] L. Li et al., "*in situ* Raman quantitative detection of methane concentrations in deep-sea high-temperature hydrothermal vent fluids", *J. Raman Spectro*., 51 (2020) 2328-2337.
[7] F.G. Hamzah and H.R. Humud, "Highly sensitive detection of Raman scattering to Rhodamine 6G dyes based on SERS for roughened plasmonic nanostructures", *AIP Conf. Proc.*, 2372(1) (2021) 080021.
[8] D.F. Marc, B.M. Kawther and T.H. Kauffmann, "Raman Probe of pollutants in water: Measurement process", *4th IMEKO TC19 SYMPOSIUM* (3 Jun 2013) 27-29.
[9] O.A. Hammadi, "New technique to synthesize silicon nitride nanopowder by discharge-assisted reaction of silane and ammonia", *Mater. Res. Exp.*, 8(8) (2021) 085013.
[10] N. Buzgar, A.I. Apopei and A. Buzatu, "Romanian Database of Raman Spectroscopy", University of Cambridge – Dissemination of IT for the Promotion of Materials Science (DoITPoMS) (2009).
[11] F.G. Hamzah and H.R. Humud, "The Raspberry-like nanostructures (SiO2@ AgNPs) fabricated by electrical exploding wire (EEW) technique for Raman scattering enhancement", *AIP Conf. Proc.*, 2290(1) (2020) 050033.
[12] R.A. Faris, Z.F. Mahdi and M.D. Abd Husein, "Immobilised gold nanostructures on printing paper for lable-free surface-enhanced Raman spectroscopy", *IOP Conf. Ser.: Mater. Sci. Eng.*, 871(1) (2020) 012019.
[13] R.M. Taha and H.A. Jawad, "Characterization of gold coating on nanostructured CR39 polymer as SERS sensor", *Iraqi J. Laser*, 17(A) (2018) 17-22.
[14] F.J. Moaen and H.R. Humud, "Raman Scattering Enhancement by silver Nanostructures Prepared by Electrical Exploding Wire Technique", *Iraqi J. Sci.*, 63(5) (2022) 2017-2024.
[15] F.G. Hamzah and H.R. Mahmood, "Signature of Plasmonic Nanostructures Synthesised by Electrical Exploding Wire Technique on Surface-Enhanced Raman Scattering", *Iraqi J. Sci.*, 62(1) (2021) 167-179.
[16] A.M.T. Allayla, R.A. Faris and Z.F. Mahdi, "Construction of insulin-like growth factor nanocomposite biosensor by Raman spectroscopy", *Vibrat. Spectro.*, 114 (2021) 103252.
[17] C.R. Maher, "Raman Spectroscopy for Nanomaterials Characterization", *SERS Hot Spots.*, Ch. 10 (2012) 215-260.
[18] Z. Li, J. Wang and D. Li, "Applications of Raman spectroscopy in detection of water quality", *Appl. Spectro. Rev.*, 51(4) (2016) 333-357.
[19] C. Krafft, "Bioanalytical applications of Raman spectroscopy", *Anal. Bioanal. Chem.*, 378 (2004) 60-62.
[20] A. Farnsworth, G. Chirima and F. Yu, "Raman Spectroscopy: A Key Technique in Investigating Carbon-Based Materials", *Spectroscopy*, 36(8) (2021) 9-14.
[21] R.R Jones et al., "Raman Techniques: Fundamentals and Frontiers", *Nanoscale Res. Lett.*, 14(1) (2019) 231.
[22] A. Garcia-Leis, J. Vicente Garcia-Ramos and S. Sanchez-Cortes, "Silver Nanostars with High SERS Performance", *J. Phys. Chem. C*, 117(15) (2013) 7791-7795.
[23] D. Harvey, "**Instrumental Analysis**", DePauw University (LibreTexts), 258 (2023). https://chem.libretexts.org/@go/page/386418.
[24] J.L. Bishop et al., "Spectral properties of anhydrous carbonates and nitrates", *Earth Space Sci.*, 8 (2021).
[25] R. Claverie et al., "Optical Sensor for Characterizing the Phase Transition in Salted Solutions", *Sensors*, 10(4) (2010) 3815-3823.
[26] J.M. McLellan et al., "Comparison of the surface-enhanced Raman scattering on sharp and truncated silver nanocubes", *Chem. Phys. Lett.*, 427(1-3) (2006) 122-126.
[27] A.W. Jabar et al., "Plasmonic Nanoparticles Decorated Salty Paper Based on SERS Platform for Diagnostic low-Level Contamination: Lab on Paper", *Iraqi J. Laser*, 18(1) (2019) 43-49.
[28] M.J. Grand et al., "Role of localized surface plasmons in surface-enhanced Raman scattering of shape-controlled metallic particles in regular arrays", *Phys. Rev. B*, 72 (2005) 033407.
[29] D.C. Rodrigues et al., "Critical assessment of enhancement factor measurements in surface-enhanced Raman scattering on different substrates", *Phys. Chem. Chem. Phys.*, (2014) 1-9.
[30] W. Plieth et al., "Electrochemical preparation of silver and gold nanoparticles: Characterization by confocal and surface enhanced Raman microscopy", *Surf. Sci.*, 597(1-3) (2005) 119-126.

